DOI: 10.1002/chem.200600029

Ab Initio and Experimental Thermodynamic and Kinetic Study of Proton-Assisted Bond Activation in Gaseous Hydrocarbons: Deconvolution of Reaction Efficiencies in the Case of Adamantane**

Juan Z. Dávalos,*[a] Rebeca Herrero,[a] Esther Quintanilla,[a, b] Pilar Jiménez,[a] Jean-François Gal,[c] Pierre-Charles Maria,[c] and José-Luis M. Abboud*[a]

Abstract: 1) Protonation at all possible sites of adamantane ($C_{10}H_{16}$) was studied at the MP2/6-311++G(3df,2p)//MP2/6-311++G(d,p) level. This provided values of the changes in the thermodynamic state functions for these processes. Whenever direct comparison was possible, the agreement with experimental data was very good. 2) By the same means, the reaction paths linking the various species obtained in these reactions were analyzed. 3) Fourier transform ion cyclotron resonance (FT-ICR) spectroscopy was used to determine the rate constants for proton transfer from 16 protonated reference bases to adamantane in the gas phase. Also, the rate constants for the formation of ionic products in these reactions were determined. 4) The experimental reaction rates were successfully predicted and refined on the basis of a simple mechanistic model based on the reaction profiles indicated above. 5) Our results hint at the potential usefulness of this approach for mechanistic studies.

Keywords: ab initio calculations · hydrocarbons · ion–molecule reactions · kinetics · protonation

Introduction

The protonation of aliphatic and alicyclic hydrocarbons, both in the gas phase and in solution, has attracted attention for several decades. Benchmark gas-phase protonation studies in this field are those of Tal'roze and Lubyumova[1] on methane, followed by seminal experiments on large linear alkanes by Field et al.,[2,3] and smaller linear and branched alkanes by Hiraoka and Kebarle.[4–6] Classical studies by Olah et al.[7] and Hogeveen[8] on the protonation of aliphatic hydrocarbons in superacids date back to the late 1960s and early 1970s. A few years ago, Fokin, Schreiner et al.[9] studied experimentally and computationally the activation of moderately strong C–C and tertiary C–H bonds in cage hydrocarbons such as adamantane ($C_{10}H_{16}$, **1**H) by weak to moderately strong electrophiles and strongly oxidizing species. All of these processes are fundamental to understanding the activation of C–H and C–C bonds.[10] We have also dealt with bond activation through protonation of organic species RX (X = halogen, OH, OMe) as a source of carbenium ions R^+.[11]

Quantum-mechanical methods are extremely valuable ("sometimes mandatory") tools for the treatment of gas-phase ion–molecule reactions.[12] Because of their relevance to our present work, we mention relatively recent studies on the protonation of propane[13] and isobutane.[14]

In 2001, Esteves, Mota et al reported the results of an ab initio study (at the MP2(full)/6-31G(d,p) level, without frequency calculations at correlated levels) on the structure and energetics of the possible species obtained by protona-

[a] Dr. J. Z. Dávalos, Dipl.-Chem. R. Herrero, Dr. E. Quintanilla, Dr. P. Jiménez, Prof. Dr. J.-L. M. Abboud
Instituto de Química Física Rocasolano, CSIC
C/Serrano 119, 28006, Madrid (Spain)
Fax: (+34) 91-564-2431
E-mail: jlabboud@iqfr.csic.es

[b] Dr. E. Quintanilla
Laboratorium für Organische Chemie
ETH Hönggerberg-HCI G 206, 8093, Zürich (Switzerland)

[c] Prof. Dr. J.-F. Gal, Prof. Dr. P.-C. Maria
Laboratoire de Radiochimie, Sciences Analytiques et Environnement
Université de Nice-Sophia Antipolis
Parc Valrose. 06108 Nice Cedex 2 (France)

[**] Work by E. Q. and R. H. was supported by pre-doctoral scholarships from the Spanish DGES. The overall project was supported by grant BQU2003-05827 from the Spanish DGICYT.

Supporting information for this article is available on the WWW under http://www.chemeurj.org/ or from the author.

tion of **1**H.[15] Their results, as well as our longstanding involvement in the study of the stability of adamantyl derivatives, including neutral compounds[16] and cations (1- and 2-adamantyl, respectively, 1-Ad$^+$ and 2-Ad$^+$),[11,17] generated our interest in the protonation of **1**H.

Herein we present the results of a computational and experimental study on this process. Because protonation can occur on several sites of the adamantane molecule, we determined the structure and thermodynamic state functions for the various protonated adamantane isomers at the MP2/6-311++G(3df,2p)//MP2/6-311++G(d,p)level of theory.[18] This information was then used to predict the kinetics of proton transfer from sixteen protonated reference bases $B_{ref}H^+$ to **1**H. These reactions were studied experimentally by means of Fourier transform ion-cyclotron resonance (FT-ICR) spectroscopy.[19] We compare the predicted and experimental data and discuss some mechanistic implications of the results.

Experimental and Methods Section

Computational details: Calculations were carried out using the computer program packages Gaussian 98[20] and Gaussian 03.[21]

The **1**H molecule presents two different H- and C-protonation sites and only one kind of C–C sites. First, the structures of the species obtained by H, C, and C–C protonation of **1**H were optimized at the MP2/6-31G(d,p) level. The possible reaction pathways linking these structures were explored at the same level by means of the QST3 method.[22] The various structures identified as stationary points on the potential energy surface of the (**1**H,H$^+$) manifold, that is, the set of different isomeric structures of protonated adamantane, were refined and their harmonic vibrational frequencies determined at the MP2/6-311++G(d,p) level. Finally, single-point energy calculations on these optimized structures were performed at the MP2/6-311++G(3df,2p) level. Raw computational energetic results and optimized structures are available as Supporting Information.

To our knowledge, no empirical correction factors for anharmonicity effects, suitable for the zero-point vibrational energy (ZPVE), vibrational contribution to the molar heat capacity at constant volume C_V, and entropy $S°_{298}$, are available for MP2/6-311++G(d,p) harmonic vibrational frequencies.[23a] This is most unfortunate, because some of the "bonds" in the protonated species have very low vibrational frequencies which contribute significantly to the heat capacity and entropy, and thus need to be accurately known. We have attempted to obviate this difficulty by using the following method.

Harmonic vibrational wavenumbers for cognate species, namely, **1**H, 1-Ad$^+$, 2-Ad$^+$, and (*tert*-C_4H_9···H_2)$^+$ were determined at both the MP2/6-31G(d) and MP2/6-311++G(d,p) levels (see Supporting Information). The linear correlations between the data obtained at both levels allowed us to estimate the MP2/6-31G(d) harmonic vibrational wavenumbers for the various species. To these values, the corrections of Radom and Scott[23] were applied and used for the estimation of the corresponding enthalpies H_{298} and Gibbs energies G_{298}. In three species (**1**H_{2a}^+, **1**H_{2b}^+, **1**H_{2c}^+, see below), the frequencies of the two torsional modes of the HH moieties are very low (see Supporting Information). Therefore, we took their total contributions to ZPVE, C_V, and $S°_{298}$ as equal to those pertaining to a freely rotating dihydrogen molecule, namely, 0.592 kcal mol^{-1} (RT), 1.984 cal mol^{-1} K^{-1} (R), and 3.15 cal mol^{-1} K^{-1}.[24] We estimate the uncertainties originating in this treatment of low-frequency modes at about 0.7 kcal mol^{-1} (for details, see Supporting Information).

Experimental section: All products were commercial and of the highest purity available. Adamantane (Aldrich) was sublimed twice. Malononitrile (Fluka) was sublimed twice. Methyl trifluoroacetate (Aldrich) contained a trace of ethyl trifluoroacetate, which was removed by distillation through a Perkin Elmer adiabatic spinning-band annular still (100 theoretical plates). $(CF_3)_2CHOH$ was stored over and distilled from P_4O_{10}. All other products (Aldrich) were used without further purification. Methane (99.999%) was obtained from Praxair. It was passed through a copper coil cooled with liquid nitrogen. Argon (≥99.998%) was obtained from Aldrich, and helium (≥99.999%) from Air Liquide.

The study was performed on a modified Bruker CMS-47 FT-ICR mass spectrometer already used in previous studies.[11g,25] The spectra were acquired by using an IonSpec Omega Data Station (IonSpec Corp., Irvine, CA).

Mixtures of **1**H (nominal pressure in the range 5×10^{-9} to 1.5×10^{-7} mbar) and a reference base B_{ref} (nominal pressures in the range $(1–5)\times10^{-7}$ mbar) were introduced into the high-vacuum section of the instrument. Argon or helium (pressure between 6×10^{-7} and 2×10^{-6} mbar) was added in all cases. Electron ionization (nominal energy below 20 eV) of the gaseous mixtures generally led to the formation of $B_{ref}H^+$. In a few cases, methane was added as proton source. Ions were allowed to cool for periods of about 5 s and then $B_{ref}H^+$ was selected by using broadband pulses and soft ejection shots. The temperature of the cell, as measured with a platinum resistor was 323 K.

Gauge sensitivities S_r relative to N_2 for the various B_{ref} were obtained according to Bartmess and Georgiadis,[26] by using for each compound the polarizability α(ahc), calculated by Miller's method.[27] The relative gauge sensitivity of **1**H was experimentally determined at the FT-ICR laboratory of the Nice-Sophia Antipolis University by using a Leybold VISCOVAC VM 210 spinning-rotor viscosity gauge.[28] The value obtained (7.89 ± 0.32) agrees within 4% with that (7.58) estimated by the Bartmess–Georgiadis method.

The decay of the abundances of these ions was monitored for times ranging from 5 to 100 s, depending on the system. At the same time, the growth of the ion signals at m/z 135 (1-Ad$^+$ and 2-Ad$^+$), 136 (^{13}C isotopomers of these ions), and 137 (protonated **1**H and ^{13}C isotope peaks of 1-Ad$^+$ and 2-Ad$^+$) were monitored.

Abstract in Spanish: *1) Se ha estudiado la protonación de todos los posibles centros básicos del hidrocarburo adamantano ($C_{10}H_{16}$) al nivel MP2/6-311++G(3df,2p)//MP2/6-311++G(d,p) y se han obtenido valores de las variaciones de funciones termodinámicas de estado para los procesos mencionados. Se ha encontrado una excelente concordancia, en los casos en los que ha podido compararse con datos experimentales. 2) Se ha aplicado el mismo método al estudio de los mecanismos de reacción que enlazan las distintas especies formadas. 3) Se han determinado las constantes de velocidad de transferencia protónica, en fase gaseosa, con 16 bases de referencia protonadas al adamantano, utilizando la Resonancia Ciclotrónica de Iones con Transformada de Fourier. 4) Se han predicho y optimizado con éxito las velocidades de reacción, utilizando un modelo sencillo basado en los perfiles de reacción indicados más arriba. 5) Los resultados obtenidos sugieren que la metodología aplicada puede ser útil para estudios mecanísticos.*

Computational Results

Energy minima: We found four stable structures for protonated adamantane on the potential energy surface of the (**1**H,H$^+$) system: three weakly bound adducts between H_2

and the adamantyl ion ($\mathbf{1}H_2^+{}_a$, $\mathbf{1}H_2^+{}_b$ and $\mathbf{1}H_2^+{}_c$), and one C-adamantonium ion ($\mathbf{1}H_2^+{}_d$) formed by protonation of a C–C bond (between C1 and C2, Figure 1). These species (Figure 2) are formed through reactions (1x) where x = a–d.

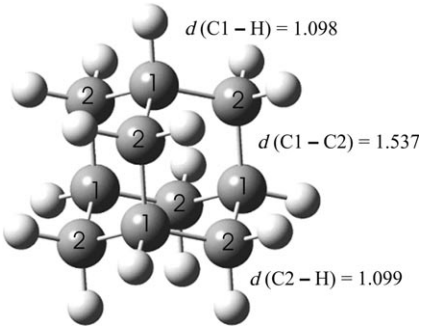

Figure 1. The structure of adamantane (**1**H) as optimized at the MP2/6-311++G(d,p) level (bond lengths in Å). Equivalent secondary and tertiary carbon atoms are numbered 2 and 1, respectively.

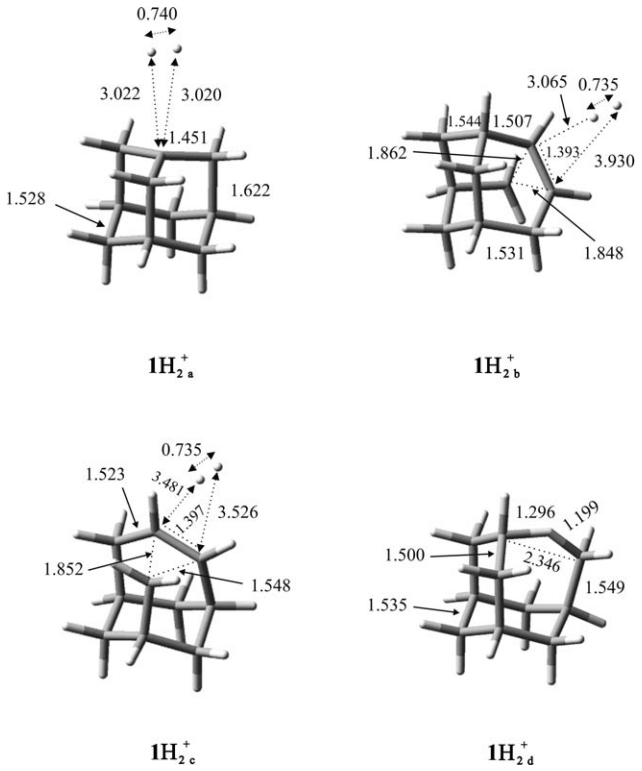

$\mathbf{1}H_{2a}^+$ $\mathbf{1}H_{2b}^+$ $\mathbf{1}H_{2c}^+$ $\mathbf{1}H_{2d}^+$

Figure 2. The four stable structures formed by protonation of adamantane: $\mathbf{1}H_2^+{}_a$, $\mathbf{1}H_2^+{}_b$, $\mathbf{1}H_2^+{}_c$ and $\mathbf{1}H_2^+{}_d$. Bond lengths (Å) obtained at the MP2/6-311++G(d,p) level.

$$\mathbf{1}H + H^+ \rightarrow \mathbf{1}H_2^+{}_x \quad \Delta_r H^\circ{}_m(1x),\ \Delta_r G^\circ{}_m(1x) \qquad (1x)$$

Species $\mathbf{1}H_2^+{}_a$ is a van der Waals (ion–dipole-induced) complex between 1-adamantyl cation and dihydrogen, while $\mathbf{1}H_2^+{}_b$ and $\mathbf{1}H_2^+{}_c$ are two isomeric, nearly degenerate complexes between 2-adamantyl cation and dihydrogen. Our results strongly support those reported in ref. [15]. Ion $\mathbf{1}H_2^+{}_c$ was not described in this reference, however. A more detailed analysis of the origins of these species is given below.

Reliable experimental standard enthalpies of formation are available for **1**H, 1-Ad^+,[29,30] and 2-Ad^+[11g] in the gas phase. This allows us to compare computational and experimental data for reactions (2a) and (2b).

$$\mathbf{1}H + H^+ \rightarrow 1\text{-}Ad^+ + H_2 \quad \Delta_r H^\circ{}_m(2a),\ \Delta_r G^\circ{}_m(2a) \qquad (2a)$$

$$\mathbf{1}H + H^+ \rightarrow 2\text{-}Ad^+ + H_2 \quad \Delta_r H^\circ{}_m(2b),\ \Delta_r G^\circ{}_m(2b) \qquad (2b)$$

The calculated results (Table 1) show excellent agreement with the experimental data and thus lend credence to the results obtained in cases where the available data are only computational. In this and other tables, the reported values of $\Delta_r H^\circ{}_m$ and $\Delta_r G^\circ{}_m$ are computed at the standard temperature of 298.15 K. We also report $\Delta_r E_m$, the electronic-plus-nuclear change in the process. This is the change in energy without inclusion of the translational, rotational and vibrational contributions.

Table 1. Experimental and calculated[a] values of the standard enthalpy, Gibbs energy, and electronic-plus-nuclear energy changes [kcal mol^{-1}] for reactions (2a) and (2b).

Reaction	$\Delta_r H^\circ{}_m$(calcd)	$\Delta_r H^\circ{}_m$(exptl)	$\Delta_r G^\circ{}_m$(calcd)	$\Delta_r E_m$(calcd)
2a	−171.5	−171.4 ± 0.9[b,c]	−173.9	−170.7
2b	−161.0	−161.7 ± 1.4[b,d]	−164.3	−160.3

[a] MP2/6-311++G(3df,2p)//MP2/6-311++G(d,p) values. [b] Using $\Delta_f H^\circ{}_m[\mathbf{1}H(g)] = -31.95 \pm 0.89$ kcal mol^{-1}.[29] [c] $\Delta_f H^\circ{}_m[1\text{-}Ad^+(g)] = 162.3 \pm 0.3$ kcal mol^{-1}, from ref. [30] and references therein. [d] $\Delta_f H^\circ{}_m[2\text{-}Ad^+(g)] = 171.9 \pm 1.1$ kcal mol^{-1}, from ref. [11g] and references therein.

The changes in the standard thermodynamic state functions for reactions (1a)–(1d) computed at this level are summarized in Table 2.

Table 2. Calculated[a] values of the standard enthalpy, Gibbs energy, and electronic-plus-nuclear energy changes [kcal mol^{-1}] for reactions (1a)–(1d).

Reaction	$\Delta_r H^\circ{}_m$(calcd)	$\Delta_r G^\circ{}_m$(calcd)	$\Delta_r E_m$(calcd)
$\mathbf{1}H + H^+ \rightarrow \mathbf{1}H_2^+{}_a$ (1a)	−171.0	−169.8	−171.7
$\mathbf{1}H + H^+ \rightarrow \mathbf{1}H_2^+{}_b$ (1b)	−160.6	−159.8	−161.4
$\mathbf{1}H + H^+ \rightarrow \mathbf{1}H_2^+{}_c$ (1c)	−160.6	−159.8	−161.4
$\mathbf{1}H + H^+ \rightarrow \mathbf{1}H_2^+{}_d$ (1d)	−162.0	−157.0	−165.4

[a] MP2/6-311++G(3df,2p)//MP2/6-311++G(d,p) values.

Formally, species $\mathbf{1}H_2^+{}_a$ (the most stable of all four), $\mathbf{1}H_2^+{}_b$, and $\mathbf{1}H_2^+{}_c$ are products of H protonation of **1**H. $\mathbf{1}H_2^+{}_d$ is an adamantonium ion, generated by C protonation of a C–C bond. Interestingly, the ranking of stabilities of these ions depends on the energetic criterion chosen. Thus, in terms of $\Delta_r E_m$ or $\Delta_r H^\circ{}_m$, the order in stability is $\mathbf{1}H_2^+{}_a > \mathbf{1}H_2^+{}_d > \mathbf{1}H_2^+{}_b \approx \mathbf{1}H_2^+{}_c$, but $\mathbf{1}H_2^+{}_a > \mathbf{1}H_2^+{}_b \approx \mathbf{1}H_2^+{}_c > \mathbf{1}H_2^+{}_d$ in terms

of $\Delta_r G°_m$. This situation reflects the fact that the van der Waals adducts have appreciably larger molar entropies (but lower zero-point vibrational energies) than the C-adamantonium ion. This is a consequence of the looseness of the complexes leading to five vibrational modes of low frequency (see Supporting Information).

Reaction (3a) is the decomposition of ion $\mathbf{1}H_2^+{}_a$ to yield 1-adamantyl cation and dihydrogen.

$$\mathbf{1}H_2^+{}_a \rightarrow 1\text{-}Ad^+ + H_2 \quad \Delta_r E_m, \Delta_r H°_m, \Delta_r G°_m \tag{3a}$$

The quantities $\Delta_r E_m$(3a), $\Delta_r H°_m$(3a), and $\Delta_r G°_m$(3a) can be obtained from the data for reactions (1a) and (2a). They are found to respectively amount to 1.1, −0.4, and −4.5 kcal mol^{-1}. This implies that, while the interaction between the 1-adamantyl and dihydrogen moieties in $\mathbf{1}H_2^+{}_a$ is feebly stabilizing, population of the vibrational levels at 298 K favors its dissociation. A similar situation prevails in the cases of reactions (3b) and (3c).

$$\mathbf{1}H_2^+{}_b \rightarrow 2\text{-}Ad^+ + H_2 \quad \Delta_r E_m, \Delta_r H°_m, \Delta_r G°_m \tag{3b}$$

$$\mathbf{1}H_2^+{}_c \rightarrow 2\text{-}Ad^+ + H_2 \quad \Delta_r E_m, \Delta_r H°_m, \Delta_r G°_m \tag{3c}$$

Here we obtain $\Delta_r E_m(3b) = 1.1$, $\Delta_r H°_m(3b) = -0.4$, $\Delta_r G°_m = -5.0$ kcal mol^{-1} and $\Delta_r E_m(3c) = 1.1$, $\Delta_r H°_m(3c) = -0.4$, $\Delta_r G°_m(3c) = -5.0$ kcal mol^{-1}.

Consider now the protonation of **1**H by a protonated reference base $B_{ref}H^+$ [reaction (4)].

$$\mathbf{1}H + B_{ref}H^+ \rightarrow \mathbf{1}H_2^+{}_x + B_{ref} \tag{4}$$

As can be deduced from the above discussion, the products obtained depend on the acidity of $B_{ref}H^+$. More precisely, bases with a gas-phase basicity GB of 158 kcal mol^{-1} or less should be able to lead to all the stable species $1H_2^+{}_x$ mentioned above. Also, because species $\mathbf{1}H_2^+{}_x$ (x = a, b, c) can so readily decompose to yield cations 1-Ad$^+$ and 2-Ad$^+$, it is to be expected that these isomeric ions will be the main species experimentally observed. However, as shown below, it is by no means obvious that species $\mathbf{1}H_2^+{}_d$ will decompose so easily.

Transition states and reaction paths: In addition to the previous protonated adamantane structures, there are two more C-protonated species. They were also reported in reference [15] We also confirm their structures, which are shown in (Figure 3) as $\mathbf{1}H_2^+{}_e$ and $\mathbf{1}H_2^+{}_f$.

The energetics for reactions (1e) and (1f) are summarized in Table 3.

Exploration of the potential energy surfaces by the QST3 method showed that these structures are transition states linking several of the previously found stable isomers. The energetics of reactions (5) and (6) are given in Table 3 and Figure 4.

$$\mathbf{1}H_2^+{}_d \rightarrow \mathbf{1}H_2^+{}_e(TS) \rightarrow \mathbf{1}H_2^+{}_a \tag{5}$$

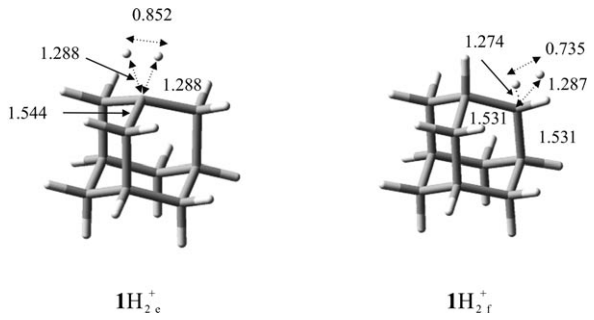

$\mathbf{1}H_2^+{}_e$ $\mathbf{1}H_2^+{}_f$

Figure 3. Structures formed by direct C protonation of **1**H (bond lengths in Å).

Table 3. Experimental and calculated[a] values of the standard enthalpy, Gibbs energy, and electronic-plus-nuclear energy changes [kcal mol^{-1}] for reactions (1e) and (1f).

Reaction	$\Delta_r H°_m$(calcd)[a]	$\Delta_r G°_m$(calcd)	$\Delta_r E_m$(calcd)
$\mathbf{1}H + H^+ \rightarrow \mathbf{1}H_2^+{}_e$ (1e)	−154.1	−148.0	−156.3
$\mathbf{1}H + H^+ \rightarrow \mathbf{1}H_2^+{}_f$ (1f)	−151.3	−145.3	−153.3

[a] MP2/6-311++G(3df,2p)//MP2/6-311++G(d,p) values.

$$\mathbf{1}H_2^+{}_d \rightarrow \mathbf{1}H_2^+{}_f(TS) \rightarrow \mathbf{1}H_2^+{}_b \tag{6}$$

Salient features of these results follow:

Reaction (5):

1) The Gibbs activation energy $\Delta_r G_m^{\neq 0}(5)$ for reaction (5) of 9.0 kcal mol^{-1} is too high to be overcome by thermal excitation at temperatures close to 298 K. However, the reaction between **1**H and $B_{ref}H^+$ may have sufficient excess energy to permit the barrier in Figure 4 to be surmounted. In this case, the final products would be the 1-adamantyl cation and dihydrogen because (as shown below) isomer $\mathbf{1}H^+{}_a$ is nearly isoenergetic with 1-Ad$^+$ + H_2.
2) Ions $B_{ref}H^+$ derived from bases with GB < 143 kcal mol^{-1} (see Tables 1 and 3) can in principle lead to direct protonation of a tertiary carbon atom. The species formed in this case is $\mathbf{1}H_2^+{}_e$, and the formation of $\mathbf{1}H_2^+{}_a$ (followed by its decomposition) would be observed again.
3) From the structural point of view, the difference in stability between $\mathbf{1}H_2^+{}_a$ and $\mathbf{1}H_2^+{}_e$ can be understood by considering the structures of **1**H and 1-Ad$^+$ (Figure 5). A salient feature is the flattening of the pyramid C1C2C2′C2″, as measured by the reduction of the angle α (Figure 5 and Table 4). This reduction originates in the nearly sp^2 hybridization of C1 in 1-Ad$^+$. In the case of $\mathbf{1}H_2^+{}_a$ the value of α is very close to that in 1-Ad$^+$. On the other hand, there is practically no difference between the α values for **1**H and $\mathbf{1}H_2^+{}_d$. In the latter case, the relatively tight bonding of the two hydrogen atoms to C1 seems to act as a source of destabilization. Indeed, the imaginary frequency (201.6 cm^{-1}) corresponds to a torsional motion of the incipient dihydrogen molecule breaking the relatively strong bond between C1 and its

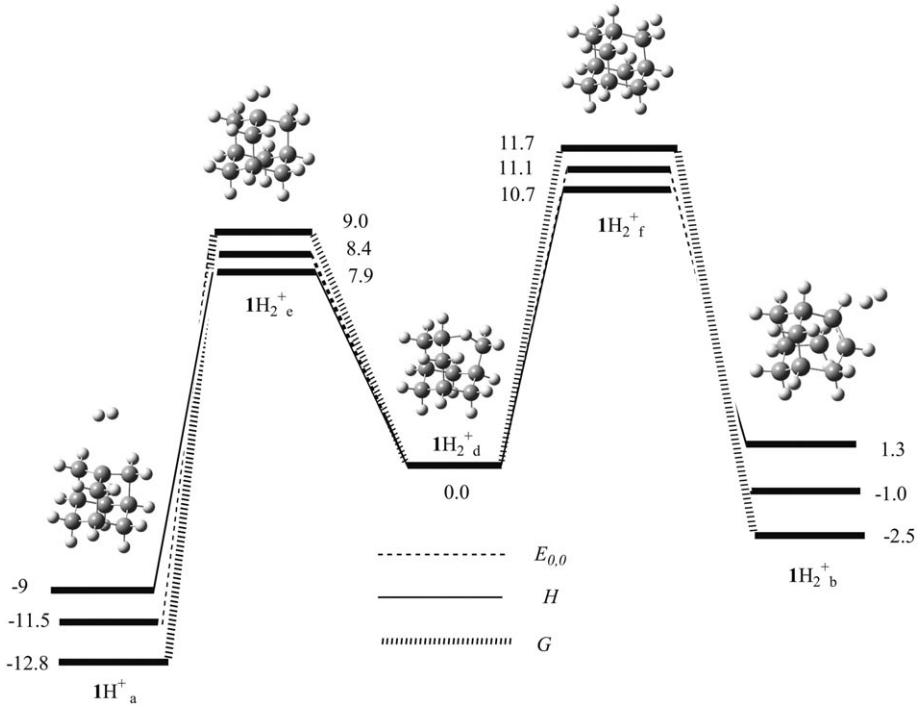

Figure 4. MP2/6-311+G(3df,2p)//MP2/6-311+G(d,p) energetics diagram of the reaction channels starting from C–C-protonated **1**H species $\mathbf{1}H_2^+{}_d$. All values in kcal mol^{-1}.

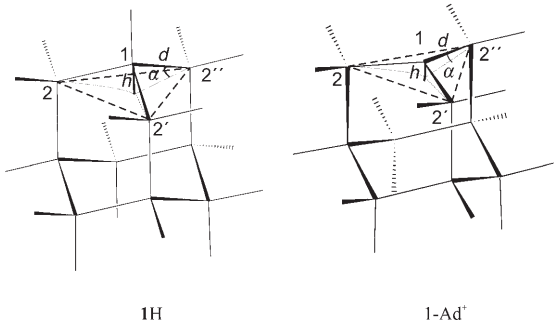

Figure 5. Definition of the angle α in adamantane hydrocarbon and 1-adamantyl cation (h is the distance from C1 to the plane defined by carbon atoms C2C2′C2″; d is the distance between C1 and any of C2, C2′, C2″).

Table 4. Values of the angle α [°] defined in Figure 5.

Species	α	Species	α
1H	19.4	$\mathbf{1}H_2^+{}_a$	8.0
$\mathbf{1}H_2^+{}_e$	16.1	1-Ad$^+$	7.9

two directly bound hydrogen atoms (C–H stretching frequencies of ca. 1900 cm^{-1}).

Overall, these results follow the same trends already found for proponium and butonium cations, that is, the van der Waals complexes of H_2 and tertiary or secondary carbenium ions are more stable than the respective tertiary or secondary H-carbenium ions.[14,15] Interestingly, it was experimentally found that the most stable structures of both protonated propane and isobutane correspond to the van der Waals (ion-induced dipole) complexes between alkyl ions and H_2.[6] Also shown was the preferential protonation in the C–C bond of *n*-alkane molecules containing 9–30 C atoms.[3] The protonation of isobutane, isopentane, and other isoalkanes in superacid media, in contrast to *n*-alkanes, gave a tertiary alkyl cation and dihydrogen as the predominant products.[7d] The present results suggest that whenever possible, protonation preferentially occurs at tertiary C–H bonds instead of C–C bonds or primary and secondary C–H bonds (and secondary C–H bonds are preferred over C–C bonds or primary C–H bonds).

Reaction (6):

1) One of the main contributors to the driving force in reaction (6) is the considerable stability of 2-Ad$^+$, a nonclassical carbenium ion portrayed in Figure 6, [31] in which the

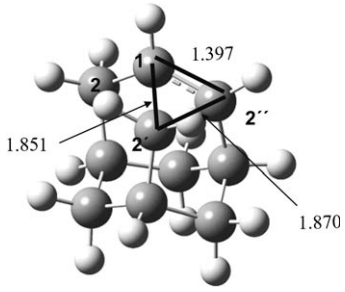

Figure 6. Optimized MP2/6-311++G(d,p) structure of 2-adamantyl cation. The nonclassical feature is highlighted.

"nonclassical feature" is emphasized by bold lines. The energetic barrier for reaction (6) is some 3 kcal mol^{-1} higher than that for reaction (5), irrespective of the energetic property taken as descriptor of stability. Thus, one can expect again that this reaction will take place only when the energy released by the formation of the collision complex is sufficient or (more likely) when the acidity of $B_{ref}H^+$ is high enough to efficiently overcome this barrier.

2) Detailed examination of the evolution from $\mathbf{1}H_2^+{}_d$ to $\mathbf{1}H_2^+{}_b$ through $\mathbf{1}H_2^+{}_f$ indicates that the hydrogen atoms constituting the dihydrogen molecule bound to 2-adamantyl cation in $\mathbf{1}H_2^+{}_b$ are those pre-existing in neutral **1**H, and that the hydrogen atom close to the corresponding secondary carbon atom in $\mathbf{1}H_2^+{}_b$ is precisely the one "trapped" between C1 and C2 in $\mathbf{1}H_2^+{}_d$.

Origins of ions $\mathbf{1}H_2^+{}_b$ and $\mathbf{1}H_2^+{}_c$: As shown in Table 2, these species are almost degenerate. They both should readily decompose to yield dihydrogen and 2-adamantyl cation. Species $\mathbf{1}H_2^+{}_b$ ultimately originates in the decomposition of $\mathbf{1}H_2^+{}_d$ formed by protonation of a C1–C2 bond. On the other hand, $\mathbf{1}H_2^+{}_c$ is formed by H protonation of a secondary hydrogen atom on the same C2 (for numbering, see Figure 1). The activation barrier for the reaction $\mathbf{1}H_2^+{}_c \rightarrow \mathbf{1}H_2^+{}_b$ amounts to 5.5 kcal mol^{-1} in terms of $\Delta_r E_m$. This value is rather high when compared to those for reactions (3b) and (3c) (essentially barrierless) and strongly suggests that species $\mathbf{1}H_2^+{}_b$ and $\mathbf{1}H_2^+{}_c$ will decompose rather than interconvert. The origin of this barrier is as follows:

Figure 2 shows that the nonclassical features of $\mathbf{1}H_2^+{}_b$ and $\mathbf{1}H_2^+{}_c$ only have one carbon atom in common, namely, the same C2 pertaining to the above-mentioned C1–C2 bond. The barrier essentially reflects the skeletal rearrangement involved in the isomerization process.

Experimental Results and Discussion

Experimental kinetic results: The experimental study of protonation reaction (4) by the above-mentioned method shows that for a given pressure of B_{ref} the rate of disappearance of $B_{ref}H^+$ cleanly follows pseudo-first-order kinetics, as given by [Eq. (8a)] where I_{BrefH+} is the intensity of the $B_{ref}H^+$ ion, and t reaction time.

$$(I_{BrefH+})_t = (I_{BrefH+})_0 \exp(-k_1 t) \quad (8a)$$

Values of k_1 were obtained as the slope of the logarithmic form of this equation. The second-order rate constants k_2 were obtained by dividing k_1 by the partial particle density (molecules cm^{-3}) of **1**H and using at least six different pressures.

Similarly, the rate of formation of the product ions with *m/z* 135 (and 136) follows pseudo-first-order kinetics, described by an expression such as Equation (8b).

$$(I_{135})_t = (I_{135})_{lim}[1-\exp(-k_2 t)] \quad (8b)$$

Representative experimental results are shown in (Figure 7), and full details are given in the Supporting Information. The experimental constants k_1 and k_2 are given in Table 5.

The ion gauge was calibrated by measuring the rate constant for reaction (9)[32,33] which is reported to be $(2.30 \pm 0.29) \times 10^{-9}$ cm^3 molecule^{-1} s^{-1}.[34]

$$[CH_3OH]^{\cdot+} + CH_3OH \rightarrow CH_3O^{\cdot} + CH_3OH_2^+ \quad (9)$$

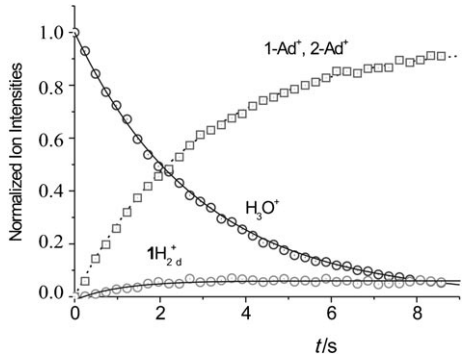

Figure 7. Example of experimental kinetic plots for the reaction between adamantane and H_3O^+. B_{ref} is H_2O. $P(\mathbf{1}H) = 7.8 \times 10^{-9}$ mbar, $P(H_2O) = 3.4 \times 10^{-7}$ mbar, $P(Ar) = 1.9 \times 10^{-6}$ mbar.

Table 5. Experimental reaction rate constants for reaction (4) and the formation of 1-Ad$^+$ and 2-Ad$^+$.

B_{ref}	GB(B_{ref})[a]	k_1[b]	ρ_1[c]	k_2[b]	ρ_2[d]
CH_4	124.4	25.3 ± 1.5	1.000 ± 0.060	24.9 ± 1.5	0.984 ± 0.060
C_2H_4[e]	155.7	19.3 ± 1.4	0.939 ± 0.066	19.6 ± 1.4	0.953 ± 0.060
$(CF_3)_2CHOH$	156.8	10.3 ± 0.5	0.919 ± 0.047	10.2 ± 0.5	0.911 ± 0.046
H_2O	157.7	18.6 ± 1.3	0.777 ± 0.053	18.1 ± 1.3	0.759 ± 0.059
C_2H_5Cl[f]	159.4	7.94 ± 0.33	0.539 ± 0.022	7.68 ± 0.31	0.522 ± 0.020
CF_3CH_2OH	160.1	5.08 ± 0.21	0.395 ± 0.016	4.84 ± 0.20	0.378 ± 0.015
1,2,3,4-$C_6H_2F_4$	160.8	3.41 ± 0.21	0.296 ± 0.017	3.32 ± 0.20	0.288 ± 0.017
CF_3COOH	162.7	3.29 ± 0.20	0.264 ± 0.016	3.23 ± 0.20	0.261 ± 0.016
$H_2C(CN)_2$	165.9	2.27 ± 0.12	0.149 ± 0.008	2.17 ± 0.11	0.156 ± 0.008
CCl_3CH_2OH	167.0	1.48 ± 0.06	0.128 ± 0.05	1.44 ± 0.09	0.124 ± 0.05
$CF_3CO_2CH_3$	169.6	0.61 ± 0.03	0.051 ± 0.02	0.60 ± 0.03	0.050 ± 0.002
$CF_3CO_2C_2H_5$	174.0	0.49 ± 0.04	0.025 ± 0.002	0.47 ± 0.03	0.024 ± 0.002
CH_3CN	178.8	0.27 ± 0.02	0.0153 ± 0.009	0.26 ± 0.02	0.0150 ± 0.009
$HCO_2C_2H_5$	183.7	0.17 ± 0.02	0.012 ± 0.001	0.16 ± 0.01	0.011 ± 0.001
CH_3COCH_3	186.9	0.071 ± 0.006	0.0047 ± 0.0004	0.070 ± 0.006	0.0047 ± 0.0004
CH_3COOCH_3	189.0	0.0046 ± 0.0009	0.0033 ± 0.0006	0.0050 ± 0.0009	0.0036 ± 0.0007

[a] From ref. [38] unless otherwise stated. [b] In units of 10^{-10} cm^3 molecule^{-1} s^{-1}. [c] Defined as $\rho = (k_1/k_{coll})/(k_1/k_{coll})_{max}$.[32a,b] [d] Defined as $\rho = (k_2/k_{coll})/(k_2/k_{coll})_{max}$.[32a,b] [e] This is formal, as ethyl cation was generated from CH_4. [f] From reference [39].

This is the average value of the experimental rate constants reported in the literature (see Supporting Information). This value is consistent with the collision rate constant $k_{coll}(4) = 2.04 \times 10^{-9}\,cm^3\,molecule^{-1}\,s^{-1}$ estimated by the ADO model.[35a] The correction factor thus derived under our working conditions was 2.43 ± 0.24 (considering a 10% uncertainty in the experimental rate constant).[35b] The observed rate constant for reaction (10) was corrected with this factor and the corresponding sensitivity factors S_r (relative to nitrogen) for methanol (1.76 ± 0.02)[36] and **1**H (7.89 ± 0.32, see above).

$$CH_5^+ + \mathbf{1}H \rightarrow CH_4 + \mathbf{1}H_2^+{}_x \qquad (10)$$

This leads to a value of $(2.53 \pm 0.26) \times 10^{-9}\,cm^3\,molecule^{-1}\,s^{-1}$, which we assume corresponds to the collision rate for this reaction $k_{coll}(10)$. The $k_{coll}(10)$ calculated on the basis of the Langevin model[35] is $2.57 \times 10^{-9}\,cm^3\,molecule^{-1}\,s^{-1}$. The experimental and calculated values are thus extremely close. Note that quadrupolar moments lead to k_{coll} values larger than those predicted by the Langevin model[37] but the high symmetry (T_d) of **1**H makes this molecule devoid of nonzero quadrupolar and octupolar moments.

The experimental results are summarized in Table 5, which lists experimental values of k_1 for reaction (4) and k_2 for the formation of ions with *m/z* 135 (and the *m/z* 136 and 137 isotopic peaks) through decomposition of $\mathbf{1}H_2^+{}_x$.

The average relative uncertainties in ρ values are estimated at 10–15% (twice the standard deviation). However, for very slow reactions, they are larger, reaching 20% for the three most basic references. Reassuringly, the experimental ρ values for k_1 and k_2 agree within 5% for all the B_{ref}. The reason is that the most abundant ions (by far under our working conditions, see below) obtained from the decomposition of the $\mathbf{1}H_2^+{}_x$ species are the isomeric 1-Ad$^+$ and 2-Ad$^+$. They have *m/z* intensities of 135 (100%), 136 (10.8%), 137 (0.06%).

Expected and observed thermokinetic pattern for protonation of 1H: Having evaluated computationally the gas-phase basicities of the different basic sites of **1**H, it is tempting to use these results to estimate its rate of protonation in the gas phase.

Consider the proton transfer between base M and reference base B_{ref} [reaction (11)].

$$M + [B_{ref}H]^+ \rightarrow [MH]^+ + B_{ref} \quad \Delta_r G^\circ{}_m(11) \qquad (11)$$

Some years ago, an important paper by Bouchoux et al.[32a] drew attention to the fact that a correlation of the form of Equation (12) is observed between the experimental rate constant for this reaction k_2 and the standard Gibbs energy change for reaction (11) $\Delta_r G°_m(11)$ [Eq. (12)], where k_{coll} is the collision rate constant, and $\Delta_r G°_a$ is an apparent activation energy for reaction (11), which is expected to be small and independent of the base B_{ref}, $\Delta_r G°_m(11)$ the difference between the gas-phase basicities of B_{ref} and M [$\Delta_r G°_m(11) = GB(B_{ref}) - GB(M)$], and ρ the "reaction efficiency" of the process.

$$\rho = k_2/k_{coll} = 1/[1 + \exp(\Delta_r G^\circ{}_m(11) + \Delta_r G^\circ{}_a)/RT] \qquad (12)$$

Although reaction (11) occurs at low pressure and thus under single-collision conditions for which a temperature cannot be maintained by gas collisions, Bouchoux et al. ascribed an effective temperature T^* to the collision complex, in a manner similar to that of Cooks[32c–e] in the kinetic method. An effective temperature of about 550 K appears to describe adequately most experimental results. Bouchoux et al. parameterized Equation (12) in terms of parameters that depend only on the properties of M and not on the nature of the base and thus suggested the use of Equation (13) as a general expression for the study of the relationship between ρ and $\Delta_r G°_m(11)$.

$$\begin{aligned}\rho &= a/[1 + \exp[b(\Delta_r G^\circ{}_m(11) + c)] \\ &= a/[1 + \exp[b(GB(B_{ref}) - GB(M) + c)]\end{aligned} \qquad (13)$$

It was found that, in general, the normalization factor a is equal to 0.90 ± 0.05 and $b = 1/RT^*$ amounts to $0.92 \pm 0.23\,kcal^{-1}\,mol$. $c = \Delta_r G°_a$ is in the range 0.6–1.4 kcal mol^{-1}.

Let us assume that GB(M) is unknown. Fitting the experimental ρ values for proton transfer from series of protonated reference bases $B_{ref}H^+$ to M through Equation (13) provides a means for its determination. This method has been quite successful, particularly when standard methods fail.[32b]

Here we apply this treatment to the protonation of adamantane by a series of reference bases B_{ref}. We use the computed values of $\Delta_r G°_m(1a)$, $\Delta_r G°_m(1b)$, $\Delta_r G°_m(1c)$, and $\Delta_r G°_m(1d)$ to estimate GB(**1**H). The previous discussion shows that **1**H acts as a molecule with different basic sites. Thus, trying to apply Equation (13) to all of them introduces such a large number of adjustable parameters that the treatment becomes meaningless. Therefore, we devised a model that considerably simplifies the situation. The basic assumptions are as follows:

1) We treat **1**H as isotropic and assume that, in principle, collisions with all hydrogen atoms and C–C bonds are equally possible. Therefore, out of 28 possible collision sites, four involve hydrogen atoms bound to tertiary carbon atoms, 12 involve hydrogen atoms bound to secondary carbon atoms, and 12 collisions will be with C–C bonds.
2) Considering that $\Delta_r G°_m(1b)$, $\Delta_r G°_m(1c)$, and $\Delta_r G°_m(1d)$ are similar, we take their average of 158.4 kcal mol^{-1} as an "average gas-phase basicity" for two of the basic sites (hydrogen atoms bound to secondary carbon atoms and C–C bonds).
3) $\Delta_r G°_m(1a)$, which describes attack at a hydrogen atom bound to a tertiary carbon atom, is 170.4 kcal mol^{-1} and is significantly different from the "average GB" value. This is taken as the second apparent basicity of **1**H.

4) Protonated bases $B_{ref}H^+$ generated from bases with GB values of less than approximately 153 kcal mol^{-1} are thus expected to react practically at collision rates with any of the basic sites of **1**H.
5) Proton donors $B_{ref}H^+$ generated from bases with GB values of about 165 kcal mol^{-1} or less will react practically at collision rates only with the hydrogen atoms bound to tertiary carbon atoms.

On account of the above, we used Equation (14) for a simplified treatment of the experimental data wherein ρ_1 and ρ_2 are respectively given by Equations (14a) and (14b).

$$\rho = \rho_1 + \rho_2 \tag{14}$$

$$\rho_1 = (6/7)/\{1 + \exp[b(\mathrm{GB}(\mathrm{B_{ref}}) - \mathrm{GB_1}(\mathbf{1H})) + c_1]\} \tag{14a}$$

$$\rho_2 = (1/7)/\{1 + \exp[b(\mathrm{GB}(\mathrm{B_{ref}}) - \mathrm{GB_2}(\mathbf{1H})) + c_2]\} \tag{14b}$$

The coefficients 6/7 and 1/7 are normalization factors (equal to 24/28 and 4/28, respectively). On account of the experimental results given in Table 3, we took $a = 1.0$. Then we optimized the values of b, $c_1 = \Delta_r G°_a$(14a), and $c_2 = \Delta_r G°_a$(14b), and found $b = 1.009 \pm 0.078$ (corresponding to $T* = 500 \pm 39$ K), $c_1 = 0.76 \pm 0.09$, and $c_2 = -0.76 \pm 0.78$ kcal mol^{-1}. These results seem quite reasonable considering the computational results and the range of usual values for $T*$. Furthermore, the magnitudes and signs of, as well as the uncertainties in, c_1 and c_2 indicate that they are consistent with processes involving low activation barriers and quite comparable to the uncertainties inherent to the estimated values of GB_1(**1**H) and GB_2(**1**H).

The ρ_1, ρ_2, and $\rho = (\rho_1 + \rho_2)$ functions displayed in Figure 8 correspond to $a = 1.0$ and to the optimized values of b, c_1, and c_2. Also presented are the experimental data points for the rates of proton transfer from the various protonated reference bases to **1**H. The correlation is rather satisfactory ($R^2 = 0.995$).

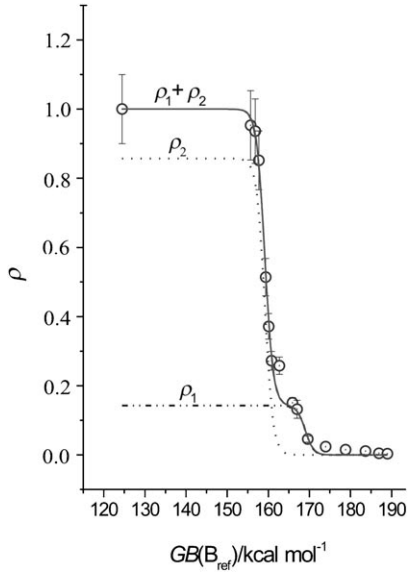

Figure 8. Plot of reaction efficiency ρ versus GB(B_{ref}) showing the deconvolution of the global observable into partial efficiencies. Experimental data and functions ρ_1, ρ_2, and $\rho_1 + \rho_2$. Values optimized are b, c_1, and c_2 (see text).

There is a formal similarity between some results of this work and the classical, time-honored reaction rate constant versus pK_a profiles.[40] They are quite useful for mechanistic studies in solution. We believe that this modified extension to the gas phase also holds some promise.

Conclusions

By using ab initio calculations, thermodynamic data for the protonation of adamantane in the gas phase were obtained. Whenever a comparison was possible, the agreement with experimental data was good.

By the same means, we have analyzed the reaction paths followed by the various species obtained in the protonation processes.

Fourier transform ICR spectrometry was used to determine the rate constants for proton transfer from 16 protonated reference bases to **1**H in the gas phase. Also determined were the rate constants for the formation of ionic products in these reactions.

The experimental reaction rates were successfully predicted (see Figure 8) according to a simple mechanistic model based on the relative basicities of the different protonation sites of adamantane and in the reaction path followed by the species thus generated.

There is a formal similarity between some results of this work and the classical, time-honored reaction rate constant versus pK_a profiles. They are quite useful for mechanistic studies in solution. We believe that this modified extension to the gas phase also holds some promise.

Acknowledgements

Valuable comments by Professors T. Baer (UNC, Chappel Hill) and J. F. Liebman (UMD, Baltimore County) are gratefully appreciated. Work by E.Q. and R.H. was supported by pre-doctoral scholarships from the Spanish DGES. The overall project was supported by grant BQU2003-05827 from the Spanish DGICYT.

[1] V. L. Tal′roze, A. K. Lyubimova, *Dokl. Akad. Nauk SSSR* **1952**, *86*, 909–915.
[2] F. H. Field, M. S. B. Munson, D. A. Becker in *Advances in Chemistry Series*, No. 58, American Chemical Society, Washington D.C., **1966**, pp. 167–192.
[3] F. H. Field, *Acc. Chem. Res.* **1968**, *1*, 42–49.
[4] K. Hiraoka, P. Kebarle, *Can. J. Chem.* **1975**, *53*, 970–972.
[5] K. Hiraoka, P. Kebarle, *J. Chem. Phys.* **1975**, *63*, 394–397.
[6] K. Hiraoka, P. Kebarle, *J. Am. Chem. Soc.* **1976**, *98*, 6119–6125.
[7] a) G. A. Olah, R. H. Schlosberg, *J. Am. Chem. Soc.* **1968**, *90*, 2726–2727; b) G. A. Olah, G. Klopman, R. H. Schlosberg, *J. Am. Chem. Soc.* **1969**, *91*, 3261–3268; c) G. A. Olah, Y. Halpern, J. Shen, Y. K. Mo, *J. Am. Chem. Soc.* **1973**, *95*, 4960–4970; d) G. A. Olah, *Angew. Chem.* **1973**, *85*, 230–311; *Angew. Chem. Int. Ed. Engl.* **1973**, *12*, 173–254.

[8] H. Hogeveen, *Recl. Trav. Chim. Pays-Bas.* **1969**, *88*, 371–378.
[9] A. A. Fokin, P. R. Schreiner, P. A. Gunchenko, S. A. Peleshanko, P. A. Shubina, S. D. Isaev, P. V. Tarasenko, N. I. Kulik, H.-M. Schiebel, A. G. Yurchenko, *J. Am. Chem. Soc.* **2000**, *122*, 7317–7326.
[10] a) A. Corma, *Chem. Rev.* **1995**, *95*, 559–614; b) J. Sommer; J. Bukkala, *Acc. Chem. Res.* **1993**, *26*, 370–375; c) J. A. Davies, P. L. Watson, J. F. Liebman, A. Greenberg, *Selective Hydrocarbon Activation, Principles and Progress*, VCH, Weinheim, **1990**; d) G. A. Olah, O. Farooq, G. K. S. Prakash, *Activation and Functionalization of Alkanes*, Wiley, New York, **1989**.
[11] a) J.-L. M. Abboud, R. Notario, E. Ballesteros, M. Herreros, O. Mó, M. Yáñez, J. Elguero, G-R. Boyer, *J. Am. Chem. Soc.* **1994**, *116*, 2486–2492; b) J.-L. M. Abboud, O. Castaño, E. W. Della, M. Herreros, P. Müller, R. Notario, J.-C. Rossier, *J. Am. Chem. Soc.* **1997**, *119*, 2262–2266; c) J.-L. M. Abboud, O. Castaño, J. Elguero, M. Herreros, N. Jagerovic, R. Notario, K. Sak, *Int. J. Mass Spectrom. Ion Processes* **1998**, *175*, 35–40; d) J.-L. M. Abboud, M. Herreros, J. S. Lomas, J. Mareda, P. Müller, J.-C. Rossier, *J. Org. Chem.* **1999**, *64*, 6401–6410; e) K. Takeuchi, M. Takasuka, E. Shiba, T. Kinoshita, T. Okazaki, J.-L. M. Abboud, R. Notario, O. Castaño, *J. Am. Chem. Soc.* **2000**, *122*, 7351–7357; f) P. Müller, J.-C. Rossier, J.-L. M. Abboud, *J. Phys. Org. Chem.* **2000**, *13*, 569–573; g) J.-L. M. Abboud, O. Castaño, J. Z. Dávalos, P Jiménez, R. Gomperts, P. Müller, M. V. Roux, *J. Org. Chem.* **2002**, *67*, 1057–1060; h) J.-L. M. Abboud, I. Alkorta, J. Z. Dávalos, P. Müller, E. Quintanilla, *Adv. Phys. Org. Chem.* **2002**, *37*, 57–135.
[12] M. Alcamí, O. Mó, M. Yáñez, *Mass Spectrom. Rev.* **2001**, *20*, 195–245.
[13] P. M. Esteves, C. J. A. Mota, A. Ramírez-Solís, R. Hernández-Lamoneda, *J. Am. Chem. Soc.* **1998**, *120*, 3213–3219.
[14] C. J. A. Mota, P. M. Esteves, A. Ramírez-Solís, R. Hernández-Lamoneda, *J. Am. Chem. Soc.* **1997**, *119*, 5193–5199.
[15] P. M. Esteves, G. G. P. Alberto, A. Ramírez-Solís, C. J. A. Mota, *J. Phys. Chem. A* **2001**, *105*, 4308–4311.
[16] a) J.-L. M. Abboud, P. Jiménez, M. V. Roux, C. Turrión, C. López-Mardomingo, G. Sanz, *J. Chem. Thermodyn.* **1992**, *24*, 217–223; b) J.-L. M. Abboud, P. Jiménez, M. V. Roux, C. Turrión, C. López-Mardomingo, *J. Chem. Thermodyn.* **1992**, *24*, 1299–1304.
[17] a) H. Flores, J. Z. Dávalos, J.-L. M. Abboud, O. Castaño, R. Gomperts, P. Jiménez, R. Notario, M. V. Roux, *J. Phys. Chem. A* **1999**, *103*, 7555–7557. b) The study of the thermodynamic stability of 1-Ad^+(g) has an important pedigree. See, for example: R. H. Staley, R. D. Wieting, J. L. Beauchamp, *J. Am. Chem. Soc.* **1977**, *99*, 5964–5972; R. Houriet, H. Schwarz, *Angew. Chem.* **1979**, *91*, 1018–1019; *Angew. Chem. Int. Ed. Engl.* **1979**, *18*, 951–952; c) The same applies to 2-Ad^+(g): C. Wesdemiotis, M. Schilling, H. Schwarz, *Angew. Chem.* **1979**, *91*, 1017–1018; *Angew. Chem. Int. Ed. Engl.* **1979**, *18*, 950–951. d) A recent, extremely thorough computational study on **1**H, 1-Ad^+, 2-Ad^+, and other species derived therefrom: G. Yan, N. R. Brinkmann, H. F. Schaeffer III, *J. Phys. Chem. A* **2003**, *107*, 9479–9485.
[18] a) J. B. Foresman, Æ. Frisch, *Exploring Chemistry with Electronic Structure Methods*, 2nd ed., Gaussian Inc, Pittsburgh, PA, **1996**, Chap. 5; b) W. J. Hehre, *A Guide to Molecular Mechanics and Quantum Chemical Calculations*, Wavefunction Inc., Irvine, **2003**, Chap. 2.
[19] a) A. G. Marshall, C. L. Hendrickson, *Int. J. Mass Spectrom.* **2002**, *215*, 59–75; b) J.-F. Gal, P.-C. Maria, E. W. Raczynska, *J. Mass. Spectrom.* **2001**, *36*, 699–716; c) J.-L. M. Abboud, R. Notario in *Energetics of Stable Molecules and Reactive Intermediates* (Ed.: M. E. Minas da Piedade), NATO Science Series C, 535, Kluwer, Dordrecht, **1999**, pp. 281–302; d) A. G. Marshall, C. L. Hendrickson, G. S. Jackson, *Mass Spectrom. Rev.* **1998**, *17*, 1–35.
[20] Gaussian 98, Revision A7, M. J. Frisch et al., Gaussian, Inc., Pittsburgh, PA, **1999** (see Supporting Information).
[21] Gaussian 03, Revision B.05, M. J. Frisch, et al., Gaussian, Inc., Pittsburgh PA, **2003** (see Supporting Information).
[22] P. Y. Ayala, H. B. Schlegel, *J. Chem.* Phys. **1997**, *107*, 375–384.
[23] a) According to our literature search and information gathered in J. Lynch, Y. Zhao, D. G. Truhlar, *Database of Frequency Scaling Factors for Electronic Structure Methods*, http://comp.chem.umn.edu/database/freq scale.htm. b) A. P. Scott, L. Radom, *J. Phys. Chem.* **1996**, *100*, 16502–16513.
[24] a) By subtracting the translational entropy ($28.08\ cal\,mol^{-1}\,K^{-1}$) at 298.15 K from the total experimental entropy of dihydrogen ($31.23\ cal\,mol^{-1}\,K^{-1}$, data from M. W. Chase, *J. Phys. Chem. Ref. Data, Monograph 9*, **1998**, 1310). b) For an extremely clear and detailed discussion of the thermodynamic consequences of hindered rotation, see N. Davidson, *Statistical Mechanics*, McGraw-Hill, New York, **1962**, Chap. 11; c) For an equally excellent treatment of *ortho*- and *para*-hydrogen and the thermodynamic properties of these species, see: N. Davidson, *Statistical Mechanics*, McGraw-Hill, New York, **1962**, Chap. 9.
[25] J.-L. M. Abboud, I. A. Koppel, I. Alkorta, E. W. Della, P. Müller, J. Z. Dávalos, P. Burk, I. Koppel, V. Pihl, E. Quintanilla, *Angew. Chem.* **2003**, *115*, 2383–2387; *Angew. Chem. Int. Ed.* **2003**, *42*, 2281–2285.
[26] J. E. Bartmess, R. M. Giorgiadis, *Vacuum* **1983**, *33*, 149–153.
[27] K. J. Miller, *J. Am. Chem. Soc.* **1990**, *112*, 8533–8542.
[28] a) J. K. Fremerey, *Vacuum* **1982**, *32*, 685–690; b) S. Dittmann, B. E. Lindenau, C. R. Tilford, *J. Vac. Sci. Technol. A* **1989**, *7*, 3356–3360; c) M. Decouzon, J.-F. Gal, S. Geribaldi, P.-C. Maria, M. Rouillard, A. Vinciguerra, *Analusis* **1986**, *15*, 471–479.
[29] H. Y. Afeefy, J. F. Liebman, S. E. Stein, *Neutral Thermochemical Data* in *NIST Standard Database No. 69*, June **2005** (Eds.: P. J. Linstrom, E. Mallard), http://webbook.nist.gov/chemistry/.
[30] Y. Li, T. Baer, *J. Phys. Chem. A* **2002**, *106*, 272–278.
[31] I. Alkorta, J.-L. M. Abboud, E. Quintanilla, J. Z. Dávalos, *J. Phys. Org. Chem.* **2003**, *16*, 546–554, and references therein.
[32] a) G. Bouchoux, J. Y. Salpin, D. Leblanc, *Int. J. Mass Spectrom.* **1996**, *153*, 37–48; b) See, for example: G. Bouchoux, J. Y. Salpin, *J. Am. Chem. Soc.* **1996**, *118*, 6516–6517; c) R. G. Cooks, T. L. Kruger, *J. Am. Chem. Soc.* **1977**, *99*, 1279–1281; d) R. G. Cooks, J. S. Patrick, T. Kotiaho, S. A. McLuckey, *Mass Spectrom. Rev.* **1994**, *13*, 287–339; e) R. G. Cooks, P. S. H. Wong, *Acc. Chem. Res.* **1998**, *31*, 379–386.
[33] T. V. Frigden, J. D. Keller, T. B. McMahon, *J. Phys. Chem. A* **2001**, *105*, 3816–3824.
[34] This is the collision rate constant k_{coll}, calculated according to the ADO model.[35]
[35] a) T. Su, M. T. Bowers in *Gas Phase Ion Chemistry, Vol. 1*, (Ed.: M. T. Bowers), Academic Press, New York, **1979**, Chap. 3, pp. 84–95, and references therein. b) As in reference [33] the correction factor is given by the ratio between the apparent rate constant for reaction (9) determined in this work and the average experimental value for the same property of $(2.30 \pm 0.29) \times 10^{-19}\ cm^3\,molecule^{-1}\,s^{-1}$.
[36] Experimental value obtained by using a spinning-rotor viscosity gauge: A. Vinciguerra, Thesis, University of Nice-Sophia Antipolis, **1987**.
[37] T. Su, M. T. Bowers in *Gas Phase Ion Chemistry, Vol. 1* (Ed.: M. T. Bowers), Academic Press, New York, **1979**, Chap. 3, pp. 108–111, and references therein.
[38] E. P. Hunter, S. G Lias, *Proton Affinity Evaluation* in *NIST Standard Database No. 69*, June **2005** (Eds.: P. J. Linstrom, W. G. Mallard), http://webbook.nist.gov/chemistry/.
[39] G. Bouchoux, F. Caunan, D. Leblanc, M. T. Nguyen, J. Y. Salpin, *ChemPhysChem* **2001**, *2*, 604–610.
[40] See, for example: a) K. J. Laidler, *Chemical Kinetics*, 3rd ed., Harper & Row, New York, **1987**, Chap. 10; b) H. Maskill, *The Physical Basis of Organic Chemistry*, Oxford University Press, New York, **1998**. Chap. 8.

Received: January 6, 2006
Published online: June 6, 2006

